

Generalized Design of Shunt Active Power Filter with Output LCL Filter

Rui Hou¹, Jian Wu¹, Yuchao Liu¹, Dianguo Xu¹

¹*Department of Electrical Engineering, Harbin Institute of Technology, Harbin 150001, P.R. China, Phone: +86 13654587937
houruihit@gmail.com*

Abstract—This paper analyses the characteristics of LCL filter in active power filter (APF) and provides an accurate formula to determine the resonant frequency of system. Based on a single-phase equivalent circuit model, a systematic approach to design APF with LCL filter is proposed. Total inductance is determined by the capability of APF. Moreover, damping ratio, resonant frequency and attenuation degree of switching ripples are the most crucial factors to design parameters of LCL filters. A method to consider them comprehensively is provided. Meanwhile, LCL filter deteriorates the compensation effect of APF. To address this problem, a novel control strategy is presented to correct the magnitude and phase of output current. Simulation and experimental results demonstrate the validity of proposed methods.

Index Terms—Damping, power harmonic filters, power quality, system analysis and design.

I. INTRODUCTION

Nowadays, the power quality in the distribution system deteriorates due to the excessive application of reactive, nonlinear and unbalanced load [1], [2]. To resolve this problem, shunt active power filter (SAPF) plays an important role and has been an area of intense investigation in recent years. Unlike passive power filter (PPF), which is sensitive to the parameters of components and apt to resonate with other loads in the grid, APF provides a flexible and rounded solution [1].

SAPF has been used extensively for harmonic suppression, reactive power compensation and grid current equilibrium in the distribution system [3], [4]. However, switching ripples produced by APF inject to the grid and result in a considerable harm. For example, capacitor loads will increase their losses and reduce service lives; moreover, high frequency noise existing in the common voltage will disturb the sensitive equipment [5]. To address this problem, switching noise filter is indispensable for APF.

Compared with L or LC filter, LCL filter ensures a better smoothing output current from APF. As a result, decreasing the inductance is easy to achieve, which guarantees the dynamic performance of APF [6]. Despite increasing the complexity, LCL filter has been widely used in medium and high power applications. Meanwhile, the design of LCL filter

is a complicated procedure and attracts much research attentions [5]–[16]. Most of literature on LCL designing is aimed at applications in grid-connected PWM rectifiers or inverters [5]–[13]. Little literature research design methods in APF applications [16]. Despite some algorithms can be references, to design LCL filters for APF is much more difficult due to the high bandwidth of output current. In ref [16], a set of methods on design, control, and implementation of LCL-filter-based SAPF are presented. Unfortunately, the part of design methods for LCL filter is not detailed.

Despite having many advantages, resonance peak of LCL filter system enlarges harmonic seriously at certain frequency, which distorts grid current and may make system unstable [16]. Fortunately, this problem can be resolved by applying damping technologies. In recent years, active damping has received lots of attention for reducing losses of system. There are several mainstream control methods for active damping. The first one is to detect the current of filter capacitor and generate a virtual damping resistor [17]–[18]. Another method is to construct an element with negative resonance peak characteristic. On one hand, some state variables can be fed back to construct notch filter element to achieve this goal [19]–[20]; on the other hand, notch filter or double band-pass filter can be applied directly to generate negative resonance peak without additional sensors [21].

Despite active damping methods have some advantages, unfortunately, the stability of system is decreased due to the function of feed-back or filter elements, which means the damping coefficient can be regulated only in a small scale to guarantee system's stability margin. Meanwhile, active methods have lower bandwidth, poor performance on dynamic response and noise immunity. Moreover, additional sensors are usually needed and the complexity of control is increased. The last but not the least, due to the restriction of system's bandwidth, effect of active damping is much inferior to corresponding passive damping [22]. Consequently, most of damping strategies in actual industrial applications adopt passive damping or combined method. Hence, it is still of positive engineering significance to research design methods for passive damping.

This paper is organized in six sections. A single-phase equivalent circuit model is established and characteristics of LCL filter system are analysed in Section II. Section III presents a set of systemic design methods for APF with LCL filter. Another contribution in Section III is providing the

relationship between damping ratio, resonant frequency and attenuation degree of switching ripples, which is used for system's generalized design. In Section IV, an improved control strategy correcting magnitude and phase for output current is proposed. Simulation and experimental results are shown in Section V to demonstrate the validity of proposed methods. Section VI concludes this paper.

II. STRUCTURE AND CHARACTERISTICS OF SYSTEM

Figure 1 shows the topology of SAPF system. SAPF consists of two basic units: one is three-phase voltage source inverter (VSI) with a capacitor in DC side, the other one is LCL output filter.

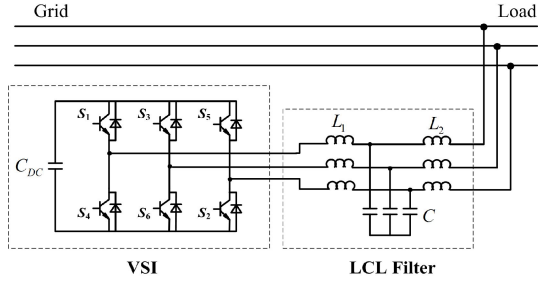


Fig. 1. Topology of SAPF system.

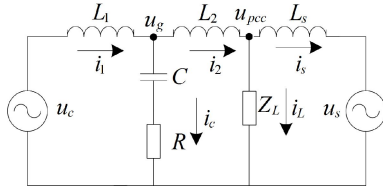


Fig. 2. Single-phase equivalent circuit.

Figure 2 shows the model of single-phase equivalent circuit. Where L_1 , L_2 and C comprise LCL output filter. u_c is the output voltage of three-phase VSI; u_s denotes the grid phase voltage. L_s , R and Z_L are respectively grid equivalent inductor, damping resistor and load. The capacitor presents a low resistance for high frequency signal, which will shunt the switching ripple current. Unlike LC filter, which require a large capacitance and is influenced by L_s seriously, LCL filter has a larger grid-side equivalent resistance and better filter performance.

No-load condition (Z_L is open circuit) is the most significant situation for analysis and design. The transfer function can be expressed by

$$G(s) = \frac{i_2}{u_c} = \frac{RCs + 1}{L_1 L_3 C s (s^2 + R \frac{L_1 + L_3}{L_1 L_3} s + \check{\zeta}_{res}^2)}, \quad (1)$$

where:

$$\check{\zeta}_{res} = \sqrt{\frac{L_1 + L_3}{L_1 L_3 C}}, \quad (2)$$

$$L_3 = L_2 + L_s, \quad (3)$$

From (1), there is an oscillating element in the transfer function. A resonant peak exists and can be weakened by

damping resistor R .

Different type of Z_L can impact upon characteristics of LCL filter system. It is not the focus of this paper; hence, some relevant conclusions are given here directly. When Z_L represents a capacitive load, extra resonant peaks will be induced; When Z_L is active resistive load, system's damping ratio can be increased and a variety of resonance is suppressed; In addition, the status of an inductive load is much the same as the condition of no load.

Considering that the current inner loop for APF usually concentrates on the current i_1 , analysis mentioned above is not applicable to the design for APF system. When system's sampling frequency and switching frequency are both equal to T_s , the transfer function of current inner loop can be approximately expressed as

$$\frac{i_1(s)}{i_1^*(s)} = \frac{1}{1.5T_s s + 1}. \quad (4)$$

The precision of current inner loop tends to be high enough, consequently, we can consider both the VSI and L_1 as a controlled current source. Furthermore, the improved single-phase equivalent circuit model is as in Fig. 3.

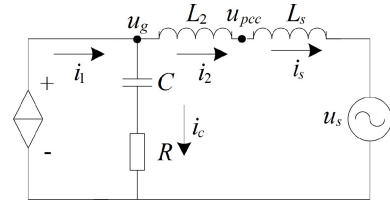


Fig. 3. Improved single-phase equivalent circuit.

In Fig. 3, considering no-load situation, the model is optimized and current transfer function is expressed as

$$G(s) = \frac{i_2(s)}{i_1(s)} = \frac{sRC + 1}{s^2 L_3 C + sRC + 1}. \quad (5)$$

From (5), the resonant frequency of system can be obtained as

$$\check{\zeta}_{res} = \sqrt{\frac{1}{L_3 C}}. \quad (6)$$

It is denoted that the resonant frequency of system depends upon total grid-side inductance L_3 with no relation to L_1 . As a matter of fact, the resonant frequency obtained from (2) is recessive due to the control strategy, whereas that from (6) is dominant and significant.

III. DESIGN METHODS OF LCL FILTER

A. Design of Total Inductance

Total inductance means the sum of L_1 and L_2 . There is a similarity between LCL filter and LC filter to design. When the inductance is low, RMS of current ripple will be biggish; whereas traceability will turn to be unsatisfactory with a high

inductance. However, the effect of LCL filter tends to be much better than LC filter. Hence, the principle consideration to design LCL filter is traceability limit. In other words, to determine the upper limit of total inductor is crucial.

For the sake of simplicity, a reduced single-phase equivalent circuit model which ignores the influence of filter capacitor is as follows in Fig. 4.

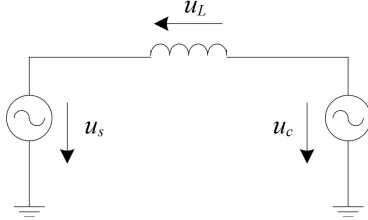


Fig. 4. Reduced single-phase equivalent circuit.

The voltage on inductor can be obtained as

$$u_L = L \frac{di_c}{dt} = u_c - u_s. \quad (7)$$

When U_{dc} denotes voltage on DC bus, output voltage of three-phase VSI u_c has five electrical levels with $0, \pm 1/3U_{dc}$ and $\pm 2/3U_{dc}$ respectively. Obviously, the worst situation for traceability of APF occurs at the peak of u_s . Without loss of generality, assumed that u_s is equal to positive peak value $\sqrt{2}U_s$, where U_s means the RMS value of grid phase voltage. An average voltage of u_c can be obtained as $0.5U_{dc}$ considering the coupling of three phases. Provided that A is the maximum slope of APF output current, the formula required is as follows

$$\frac{0.5U_{dc} - \sqrt{2}U_s}{\tilde{S}L} \geq A. \quad (8)$$

Besides, regarding fundamental wave, (8) can be converted to the following one

$$\frac{\frac{\sqrt{2}}{2}U_{dc} - U_s}{\tilde{S}_1 L} \geq A_1, \quad (9)$$

where A_1 means the maximum RMS value of APF output current for fundamental wave. We can convert harmonic to fundamental wave by multiplying relative coefficient for the sake of simplicity. Take 100 A 5th harmonic for example, it can be considered as 500 A fundamental wave. Then we can choose the maximum corrected fundamental wave to calculate total inductance.

B. Design of Damping Ratio

Grid inductance L_s can be estimated by transformer's parameters. Define κ as the damping ratio, (5) can be converted into the standard form as follows

$$G(s) = \frac{i_2}{i_1} = \frac{RCs + 1}{\frac{s^2}{\tilde{S}_{res}^2} + 2\kappa \frac{s}{\tilde{S}_{res}} + 1}, \quad (10)$$

where

$$\tilde{S}_{res} = \sqrt{\frac{1}{L_s C}}, \quad (11)$$

$$\kappa = \frac{R}{2} \sqrt{\frac{C}{L_s}}. \quad (12)$$

We can obtain the magnitude-frequency characteristic as

$$|G(j\tilde{S})| = 20[\lg \sqrt{(RC\tilde{S})^2 + 1} - \lg \sqrt{(1 - \frac{\tilde{S}^2}{\tilde{S}_{res}^2})^2 + (2\kappa \frac{\tilde{S}}{\tilde{S}_{res}})^2}]. \quad (13)$$

It is indicated that the oscillating element influences the part $\lg \sqrt{(1 - \frac{\tilde{S}^2}{\tilde{S}_{res}^2})^2 + (2\kappa \frac{\tilde{S}}{\tilde{S}_{res}})^2}$. Define $\tilde{S} = k\tilde{S}_{res}$, and the magnitude gain at the frequency of S is $-20\lg \sqrt{(1 - k^2)^2 + (2\kappa k)^2}$ dB. When $\tilde{S} \ll \tilde{S}_{res}$ or $\tilde{S} \gg \tilde{S}_{res}$, the gain is about 0 dB. Nevertheless, when $\tilde{S} = \tilde{S}_{res}$ the gain will trend to be infinity if $\kappa = 0$. When we introduce damping, the gain is $-20\lg 2\kappa$ dB and the variation tendency is as in Fig. 5.

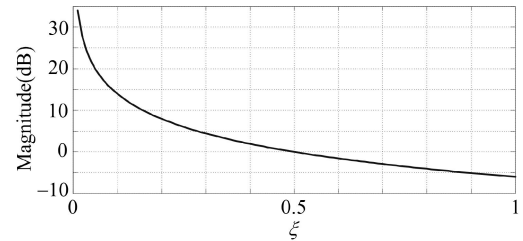


Fig. 5. Magnitude with different κ .

It is indicated in Fig. 5 that magnitude is amplified when $\kappa < 0.5$ and the larger gain the less κ . When $\kappa \geq 0.5$, no amplification occurs for the oscillating element. In this sense, we should design κ larger than 0.5. However, that will increase thermal losses of system by enlarging the value of R . If a magnification below 50% at the resonant frequency is required, κ must be larger than 0.33.

C. Design of Resonant Frequency

It is important to note that there are two typical elements with inertia differential element and oscillating element respectively. Owing to a tiny time constant, inertia differential element mainly performs a role in high frequency. While in low and medium frequency, oscillating element dominantly affects the characteristics of system. From (10), we can obtain the phase-frequency characteristic as

$$\Phi(j\tilde{S}) = \arctan(RC\tilde{S}) - \arctan\left(\frac{2\kappa\tilde{S}\tilde{S}_{res}}{\tilde{S}_{res}^2 - \tilde{S}^2}\right). \quad (14)$$

Define $\tilde{S} = k\tilde{S}_{res}$. From (13) and (14), magnitude gain and phase excursion are respectively

$$-20\lg\sqrt{(1-k^2)^2+(2\zeta k)^2} \text{ dB and } -\arctan\left(\frac{2\zeta k}{1-k^2}\right) \text{ radian.}$$

The characteristics when $\zeta = 0.5$ or $\zeta = 0.33$ and $k \leq 1$ are as in Fig. 6.

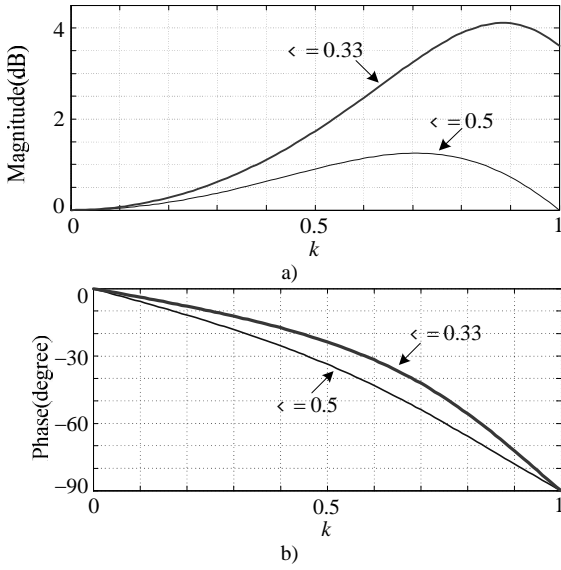


Fig. 6. Characteristics when $k \leq 1$.

From Fig. 6(a), it is indicated that magnitude is enlarged when $k \leq 1$ and a higher damping can restrain the gain better. From Fig. 6(b), it is noteworthy that phase excursion occurs across LCL filter and a higher damping leads to a more serious delay. Specifically, if $\tilde{S} = \frac{2}{3}\tilde{S}_{res}$, when $\zeta = 0.33$ magnitude reach about 3 dB which means current is enlarged by 41 %, and phase delay is 38° ; when $\zeta = 0.5$, magnitude is 1.23 dB which means current is enlarged by 15 %, and phase delay is 50° . Consequently, resonant frequency must exceed APF's compensation bandwidth by 50 % in order to reduce the adverse effect from the oscillating element.

In addition, Fig. 7 shows the magnitude characteristics when $k \geq 1$. It is indicated that magnitude characteristics tend to turn superposition for different damping. If $k = 2$, gain is -10.3 dB and -11.14 dB with $\zeta = 0.33$, $\zeta = 0.5$ respectively, which means an attenuation by 70 % at least. Hence, resonant frequency should be below half of switching frequency.

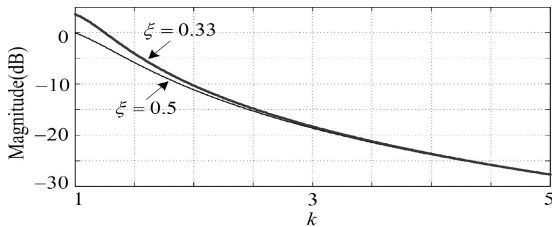


Fig. 7. Characteristics when $k \geq 1$.

D. Attenuation Degree of Switching Ripple

The chief purpose to use LCL filter is to prevent switching ripple from injecting into grid. Therefore attenuation degree of switching ripple is an important indicator to design and evaluate LCL filter.

From (10), magnitude at the switching frequency is

$$\begin{aligned} |G(j\tilde{S}_s)| &= 20[\lg\sqrt{(\tilde{S}_s RC)^2+1} - \\ &- \lg\sqrt{(\tilde{S}_s RC)^2+(1-\tilde{S}_s^2 L_3 C)^2}] < B, \end{aligned} \quad (15)$$

where \tilde{S}_s is switching frequency and B is the gain to achieve. Define attenuation degree of switching ripple as y and it can be obtained from (10) as follows

$$y = \frac{I_2(\tilde{S}_s)}{I_1(\tilde{S}_s)} = \sqrt{\frac{(\tilde{S}_s RC)^2+1}{(\tilde{S}_s RC)^2+(1-\tilde{S}_s^2 L_3 C)^2}}. \quad (16)$$

Define

$$h = \tilde{S}_{res} / \tilde{S}_s. \quad (17)$$

From (11), (12), (16) and (17) simultaneously, y can be determined uniquely by ζ and h as follows

$$y = \sqrt{\frac{1 + \frac{4\zeta^2}{h^2}}{1 + \frac{4\zeta^2}{h^2} + \left| \frac{1}{h^4} - \frac{2}{h^2} \right|}}. \quad (18)$$

A 3D graphic can be plotted as in Fig. 8.

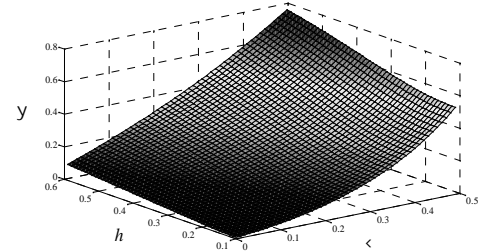


Fig. 8. 3D graphic on relationship of three factors.

From Fig. 8, it is indicated that y increases rapidly as we enhance ζ . When ζ is small, y is always low however much h is. However, when ζ is big such as 0.5, y is at least 50 % when $h = 0.1$. As a result, we usually determine ζ and h reasonably in order to reduce the value of y . In general, y should be below 0.2 to ensure the switching ripple filter effect. In some fastidious occasions, y may be chosen below 0.15.

E. Global Design Methods

How to design LCL filter in APF integrally?

To begin with, we should make certain of the capacity and application. Total inductance can be obtained from methods indicated above. The maximum value of capacitor usually is chosen below 5 % of APF's capacity. Switching frequency of APF can be determined by the capacity and heat-sinking capability which is generally below 10 kHz for actual applications. Target value of y should be chosen according to actual conditions.

Moreover, we can obtain resonant frequency and damping ratio from methods proposed above.

Last but not least, check the value of y using (18). If y is

dissatisfactory, try reducing h or ζ . ALL the parameters of LCL filter are achieved.

IV. OPTIMIZATION CONTROL METHODS

If grid load is harmonic source, the model of single-phase equivalent circuit of system is as follows as in Fig. 9.

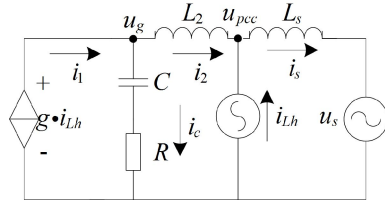


Fig. 9. Single-phase equivalent circuit.

In Fig. 9, i_{Lh} is harmonic current source. Because ideal harmonic voltage source is inexistent, practical nonlinear load can be equivalent to harmonic current source with different peaks. Compensation coefficient g is usually equal to -1.

If $i_2 = i_1 = -i_{Lh}$, harmonic will be compensated completely. Unfortunately, i_2 changes not only magnitude but also phase compared with i_1 as indicated above. Consequently, traditional feed-forward control methods which i_1 is equal to $-i_{Lh}$ cannot achieve nice effect especially when resonate frequency is low. Factually, due to a low switching frequency, this situation often occurs.

If used adequate magnitude and phase compensation to reference value of i_1 , to make $i_2 = -i_{Lh}$ can eliminate the adverse effect of LCL filter.

Harmonic can be extracted by synchronous rotating transformation methods which can easily distinguish positive-order and negative-order components from current. The schematic diagram of harmonic extraction is showed in Fig. 10.

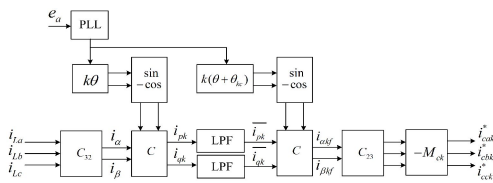


Fig. 10. Harmonic extraction methods.

Load current is transformed by Clarke and Park matrix into i_{pk} and i_{qk} which represent active harmonic current and reactive harmonic current respectively. The harmonic order k is positive value when we are to extract positive-order harmonic; k is negative value when we are to extract negative-order harmonic. θ_n is the phase angel of A-phase fundamental voltage obtained from phase-locked loop. Through Park transformation, k -order harmonic turns into DC component which can be extracted by a Low-pass filter, and the other order harmonics are transformed into AC component. Traditionally, Park inverse transformation uses the same phase information with direct transformation. Here a novel control strategy is proposed, which makes a lead compensation for Park inverse transformation. θ_{kc} is the lead angle obtained by (14). Through Clarke inverse

transformation, k -order harmonic current reference can be obtained by multiply -1 considered reference direction traditionally. Here magnitude compensation is introduced, where M_{ck} is a compensation factor obtained by (13). Through feeding forward magnitude and phase compensation, the adverse effect of LCL filter can be reduced.

V. SIMULATION AND EXPERIMENT RESULTS

Here an example to design APF with 200A capacity is provided. Filter capacitor chooses 60 uF delta connected which introduce reactive current of 12.4 A, and this meets the rule that reactive current should be below 5 % of capacity mentioned above approximately. The total inductance should be below 0.28 mH when $U_{dc} = 800V$ using the rule on total inductance. Switching frequency of system is decided to be 5 kHz for the purpose of reducing switching loss. The maximum order harmonic to compensate is 13th, and resonant frequency should be chosen between 1 kHz and 2.5 kHz according to the rule proposed above. Based on the parameter of transformer in experiment place, an estimated value of L_s is 0.04 mH. We choose $L_2 = 0.07$ mH and resonate frequency is 1.13 KHz calculated by (6). From (17), it can be obtained that $h = 0.226$. Damping ratio ζ is chosen to be 0.32 and $\gamma = 0.16$ can be obtained from (18). As a result, we can choose $L_1 = 0.2mH$, $R = 0.5\Omega$ (Y connection).

A model is established with Matlab Simulink according to parameters above. Nonlinear load adopts harmonic current source. The RMS of harmonic is shown in Table I.

TABLE I. LIST OF HARMONIC.

| | 5 th RMS(A) | 7 th RMS(A) | 11 th RMS(A) | 13 th RMS(A) | THD (%) |
|--|---------------------------|---------------------------|----------------------------|----------------------------|---------|
| Load side | 132 | 88.5 | 36 | 15 | 149.5 % |
| Grid side without correction | 5.47 | 11.64 | 11.16 | 4.76 | 15.97 % |
| With magnitude correction | 5.29 | 9.24 | 6.53 | 4.67 | 12.2 % |
| With phase correction | 5.02 | 8.73 | 7.74 | 2.96 | 12.16 % |
| With magnitude and phase correction | 4.65 | 7.93 | 3.77 | 4.00 | 10.18 % |

Firstly, resonant frequency is 1.13 KHz according to (6), whereas it is 1.41 KHz obtained from (2). A contrast of the gain is listed in Table II. It is shown that the magnification times with the (3) are much larger and validity of the proposed method to obtain resonant frequency is proved. Meanwhile, the gain is about 1.6, which is accordant to design method on damping ratio mentioned above.

Moreover, magnitude compensation factor M_{ck} and the lead angle θ_{kc} for various orders harmonic can be obtained from (13) and (14) which are listed in Table III.

TABLE II. MAGNITUDE GAIN AROUND RESONANCE FREQUENCY.

| | 1125Hz | 1150Hz | 1400Hz | 1425Hz |
|---------------|--------|--------|--------|--------|
| Peak of i_1 | 0.3 | 0.78 | 0.51 | 0.94 |
| Peak of i_2 | 0.46 | 1.26 | 0.66 | 1.08 |
| Gain | 1.53 | 1.61 | 1.29 | 1.15 |

TABLE III. MAGNITUDE AND PHASE COMPENSATION FACTOR.

| Order | 5 th | 7 th | 11 th | 13 th |
|---------------------|-----------------|-----------------|------------------|------------------|
| M_{ck} | 1/1.0503 | 1/1.1013 | 1/1.2702 | 1/1.3946 |
| μ_{kc} (radian) | 0.0071 | 0.0201 | 0.0853 | 0.1497 |

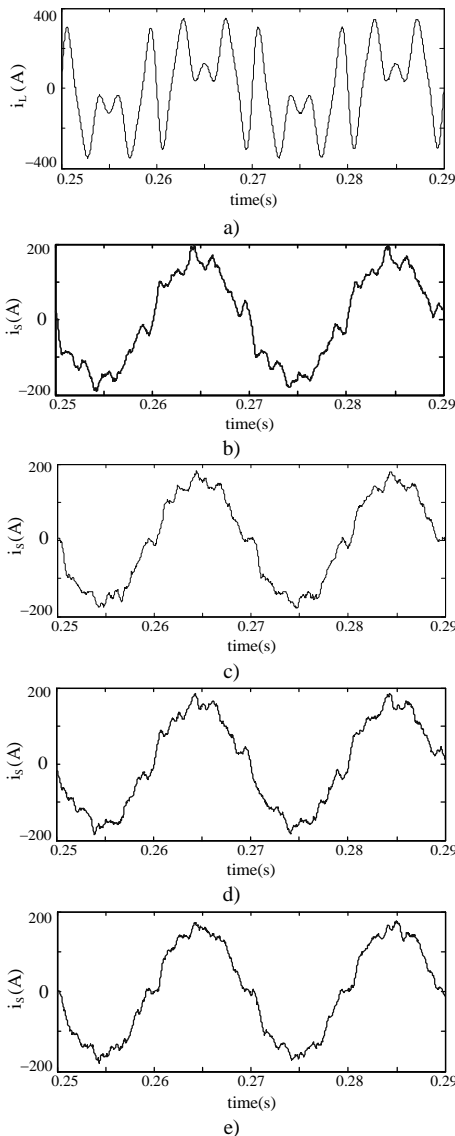


Fig. 11. Current waveforms for simulation: a) Load current; b) Grid current without correction; c) Grid current with magnitude correction; d) grid current with phase correction; e) Grid current with magnitude and phase correction.

From Fig. 11, it is indicated that load current has a serious distortion. After compensation by APF, grid current becomes approximately sinusoidal but not ideal. There are several reasons influencing compensation performance. Firstly, the harmonic RMS of load current is very large, which is a rather awful occasion and difficult to compensate by APF due to a steep changing current. Secondly, the resonant characteristics of LCL filter make APF’s output current distorted. Last but not least, the control strategy is imperfect and system’s inertial and delay elements decrease the accuracy of current tracking. On the other hand, from Table I, compensation effect is obviously improved when using correction. With individual magnitude or phase correction, THD of grid current reduces to 12.2 %, when we correct magnitude and phase, integrated compensation effect is the best during the methods provided. THD of grid current reduces to 10.18 %

and total harmonic elimination rate reaches up to 94.7 % which is very satisfactory.

To further determine the effectiveness and validity of the proposed method, an experiment is accomplished in the laboratory. Figure 12 is the photo of the laboratory prototype. As is showed, APF and thyristor switched capacitor (TSC) compose a hybrid system to compensate the reactive power and harmonic current generated by inductors and SCR rectifier loads in the grid respectively. In the experiment, only SCR rectifier loads are connected to the grid and the RMS value of harmonic current in load side is showed in Table IV. Then APF prototype with the compensation capacity of 100 KVA is switched on to verify the proposed method. Parameters of LCL filter for APF are as follows: $L_1 = 0.3\text{mH}$, $L_2 = 0.075\text{mH}$, $C=90\mu\text{F}$, $R = 0.5\Omega$ (Y connection). Inductors and capacitors in LCL filter are available in the laboratory but not with the best value, which induces the damping ratio to be only 0.15. The RMS value of grid line voltage is 380 V, and DC-side voltage for APF is 760 V accordingly. Switching frequency for APF is 5 KHz, and 5th, 7th, 11th, 13th harmonic current is selected to be compensated.

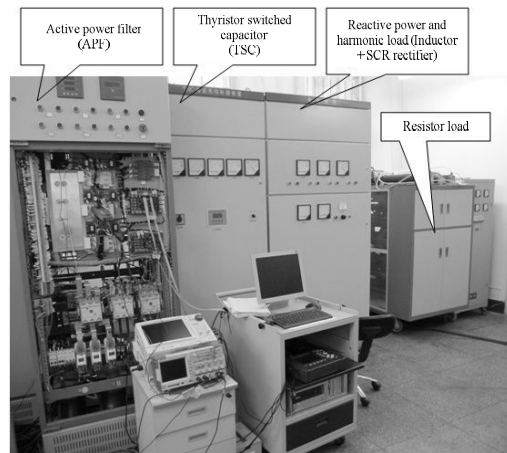


Fig. 12. Photo of Laboratory prototype.

From Fig. 13, grid current after compensation is not ideal. This is mainly because inductors and capacitors in LCL filter are existing but not with the best value, which induces the damping ratio to be only 0.15. Resonant frequency is approximately 1.5 kHz and the circumambient harmonic is enlarged obviously. Another reason is the adoption of selective harmonic compensation strategy which means only 5th, 7th, 11th, 13th harmonic is chosen. Nevertheless, it is indicated that after magnitude and phase correction grid current is more sinusoidal. From Table IV, after magnitude and phase correction harmonic elimination has a better performance for all the selected harmonics. THD of load current reaches up to 73.2 %, and THD of grid current decreases from 22.2 % to 15.1 % using the strategy proposed

TABLE IV. LIST OF HARMONIC AFTER COMPENSATION.

| | 5th | 7th | 11th | 13th |
|---------------------------|------|------|------|------|
| Load current(A) | 28.2 | 15.9 | 6.1 | 5.6 |
| Without correction | 5.1 | 3.5 | 3.8 | 3.0 |
| With correction | 2.1 | 1.6 | 2.8 | 1.6 |

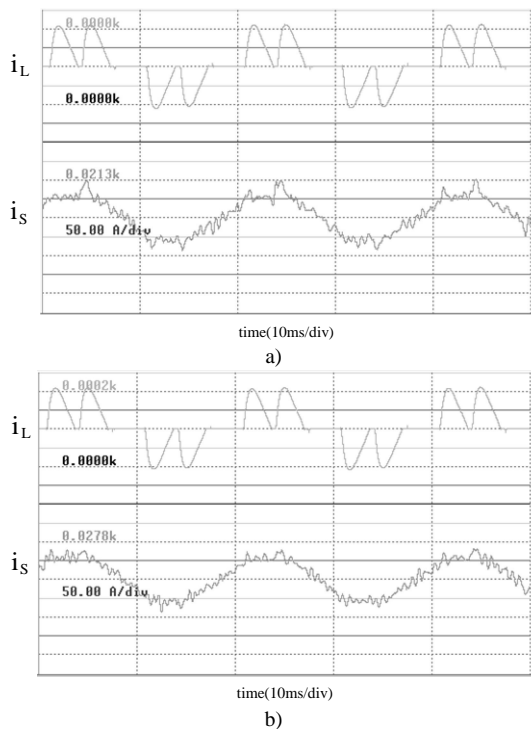


Fig. 13. Current waveforms for experiment: a) Current without correction; b) Current with correction.

VI. CONCLUSIONS

This paper has made the following conclusions on the basis of previous studies:

A single-phase equivalent circuit model has been established to analyse the characteristics of LCL filter applied in APF. Oscillating element leads to a resonance peak enlarging harmonic. Resonant frequency depends upon total grid-side inductor with no relation to inverter-side inductor owing to the function of inverter current loop.

We proposed a set of methods to design LCL filter. Total inductance is restricted by the capability of APF. Damping ratio, attenuation degree of switching ripples and resonant frequency are the crucial factors to determine the performance of LCL filter. Intrinsic relation of them has been presented and a comprehensive consideration is essential.

LCL filter has an adverse effect on magnitude and phase of compensation current. A correction method using synchronous rotating transformation has been proposed and demonstrated by simulation and experimental results. Further studies may be needed on adapting to varying parameters of system.

REFERENCES

- [1] H. Akagi, E. H. Watanabe, M. Aredes, *Instantaneous power theory and applications to power conditioning*. New Jersey, USA: John Wiley & Sons; 2007. [Online]. Available: <http://dx.doi.org/10.1002/0470118938>
- [2] M. Angulo, D. A. Ruiz-Caballero, J. Lago, M. L. Heldwein, *et al.*, "Active power filter control strategy with implicit closed-loop current control and resonant controller", *IEEE Trans. Industrial Electronics*, vol. 60, pp. 2721–2730, 2013. [Online]. Available: <http://dx.doi.org/10.1109/TIE.2012.2196898>
- [3] Xinyang Liu, Jie Wang, Gang Yao, "A novel hysteresis current control strategy with fuzzy bandwidth for active power filter", *Elektronika ir Elektrotechnika*, no. 4, pp. 3–8, 2012. [Online]. Available: <http://dx.doi.org/10.5755/j01.eee.120.4.1442>
- [4] S. Biricik, O. C. Ozerdem, S. Redif, "Performance improvement of active power filter under distorted and unbalanced grid voltage conditions", *Elektronika ir Elektrotechnika*, vol. 19, no. 1, pp. 35–39, 2013. [Online]. Available: <http://dx.doi.org/10.5755/j01.eee.19.1.3247>
- [5] M. Liserre, F. Blaabjerg, S. Hansen, "Design and control of LCL-filter-based three-phase active rectifier", *IEEE Trans. Industrial Applications*, vol. 41, pp. 1281–1291, 2005. [Online]. Available: <http://dx.doi.org/10.1109/TIA.2005.853373>
- [6] Guo Xizheng, You Xiaojie, Li Xinran, Hao Ruixiang, Wang Dewei, "Design method for the LCL filters of three-phase voltage source PWM rectifiers", *Journal of power electronics*, vol. 12, pp. 559–566, 2012.
- [7] J. Dannehl, C. Wessels, F. W. Fuchs, "Limitations of voltage-oriented PI current control of grid-connected PWM rectifiers with LCL filters", *IEEE Trans. Industrial Electronics*, vol. 59, pp. 380–388, 2009. [Online]. Available: <http://dx.doi.org/10.1109/TIE.2008.2008774>
- [8] Zhixiang Zou, Zheng Wang, Ming Cheng, "Modeling, analysis, and design of multifunction grid-interfaced inverters with output LCL filter", *IEEE Trans. Power Electronics*, vol. 29, pp. 3830–3839, 2014. [Online]. Available: <http://dx.doi.org/10.1109/TPEL.2013.2280724>
- [9] K. Jalili, S. Bernet, "Design of LCL filters of active-front-end two-level voltage-source converters", in *IEEE Trans. Industrial Electronics*, vol. 56, pp. 1674–1689, 2009. [Online]. Available: <http://dx.doi.org/10.1109/TIE.2008.2011251>
- [10] Weimin Wu, Yuanbin He, Tianhao Tang, F. Blaabjerg, "A new design method for the passive damped LCL and LLCL filter-based single-phase grid-tied inverter", *IEEE Trans. Industrial Electronics*, vol. 60, pp. 4339–4350, 2013. [Online]. Available: <http://dx.doi.org/10.1109/TIE.2012.2217725>
- [11] I. J. Gabe, V. F. Montagner, H. Pinheiro, "Design and implementation of a robust current controller for VSI connected to the grid through an LCL filter", *IEEE Trans. Power Electronics*, vol. 24, pp. 1444–1452, 2009. [Online]. Available: <http://dx.doi.org/10.1109/TPEL.2009.2016097>
- [12] Huichun Huang, Renjie Hu, Guiping Yi, "Research on dual-loop controlled grid-connected inverters on the basis of LCL output filters", *Elektronika ir Elektrotechnika*, vol. 20, no. 1, pp. 8–14, 2014. [Online]. Available: <http://dx.doi.org/10.5755/j01.eee.20.1.5589>
- [13] M. Pastor, J. Dudrik, "Design of output LCL filter for 15-level cascade inverter", *Elektronika ir Elektrotechnika*, vol. 19, no. 8, pp. 45–48, 2013. [Online]. Available: <http://dx.doi.org/10.5755/j01.eee.19.8.5394>
- [14] J. Muhlethaler, M. Schweizer, R. Blattmann, J. W. Kolar, *et al.*, "Optimal design of LCL harmonic filters for three-phase PFC rectifiers", *IEEE Trans. Power Electronics*, vol. 28, pp. 3114–3125, 2013. [Online]. Available: <http://dx.doi.org/10.1109/TPEL.2012.2225641>
- [15] Wang Yaoqiang, Wu Fengjiang, Sun Li, Sun Kui, "Optimized design of LCL filter for minimal damping power loss", *Proc. CSEE*, vol. 27, pp. 90–95, 2010.
- [16] Tang Yi, Poh Chiang Loh, Wang Peng, Fook Hoong Choo, Gao Feng, F. Blaabjerg, "Generalized design of high performance shunt active power filter with output LCL filter", *IEEE Trans. Industrial Electronics*, vol. 3, pp. 1443–1452, 2012.
- [17] Xiaohu Zhou, Jiwei Fan, A. Q. Huang, "High-frequency resonance mitigation for plug-in hybrid electric vehicles' integration with a wide range of grid conditions", *IEEE Trans. Power Electronics*, vol. 27, pp. 4459–4471, 2012. [Online]. Available: <http://dx.doi.org/10.1109/TPEL.2012.2185833>
- [18] Yunwei Li, "Control and resonance damping of voltage-source and current-source converters with LC filters", *IEEE Trans. Industrial Electronics*, vol. 56, pp. 1511–1521, 2009. [Online]. Available: <http://dx.doi.org/10.1109/TIE.2008.2009562>
- [19] J. Dannehl, M. Liserre, F. W. Fuchs, "Filter-based active damping of voltage source converters with LCL filter", *IEEE Trans. Industrial Electronics*, vol. 8, pp. 3623–3633, 2011. [Online]. Available: <http://dx.doi.org/10.1109/TIE.2010.2081952>
- [20] M. Hanif, V. Khadkikar, Weidong Xiao, J. L. Kirtley, "Two degrees of freedom active damping technique for LCL filter-based grid connected PV systems", *IEEE Trans. Industrial Electronics*, vol. 61, pp. 2795–2803, 2014. [Online]. Available: <http://dx.doi.org/10.1109/TIE.2013.2274416>
- [21] M. Liserre, A. Dell'Aquila, F. Blaabjerg, "Genetic algorithm-based design of the active damping for an LCL-filter three-phase active rectifier", *IEEE Trans. Power Electronics*, vol. 1, pp. 76–86, 2004. [Online]. Available: <http://dx.doi.org/10.1109/TPEL.2003.820540>
- [22] N. Mukherjee, D. De, "Analysis and improvement of performance in LCL filter-based PWM rectifier/inverter application using hybrid damping approach", *IET Power Electronics*, vol. 6, pp. 309–325, 2013. [Online]. Available: <http://dx.doi.org/10.1049/iet-pel.2012.0032>